Interdisciplinary Research in Medical Sciences Specialty
ISSN: 3062-4401
2026, Volume 6, Issue 1, Page No: 15-28

Available online at: www.galaxypub.co/page/journals

Galaxy Publication

Artificial Intelligence–Enabled Cardiac Lesion Quantification Improves Diagnosis of Sudden Cardiac Death

Wouter De Smet[1]*, Liesbeth Van Dam[1], Pieter Janssens[2]

[1]Department of Forensic Pathology and AI Diagnostics, Faculty of Medicine, KU Leuven, Leuven, Belgium.
[2]Department of Cardiac Pathology and Machine Learning, Faculty of Medicine, Ghent University, Ghent, Belgium.

***E-mail** ✉ wouter.desmet@kuleuven.be

Received: 16 November 2025; **Revised:** 28 January 2026; **Accepted:** 02 February 2026

ABSTRACT

Preventing sudden cardiac death (SCD) in clinical settings and establishing it accurately in forensic investigations remain difficult because of the lack of uniform quantitative standards for assessing morphological and histopathological changes in the heart. This study aimed to create a machine learning-powered system for evaluating cardiac lesions, thereby enabling more precise quantitative diagnosis and risk assessment of SCD. The investigation incorporated 2284 adult autopsy cases from the forensic center at Sun Yat-sen University together with 1883 cases from five independent external centers to construct and validate a diagnostic model based on postmortem findings. Eight different machine learning algorithms were tested, and the superior model underwent additional assessment through human–machine collaboration experiments. This model was subsequently adapted to detect myocardial infarction within a prospective clinical group of 204 individuals who presented with chest pain. Cases of SCD displayed markedly increased right ventricular wall thickness (OR: 1.17 [95% CI: 1.04–1.32] per mm) along with enlarged valve annulus circumferences for the tricuspid (OR: 1.17 [95% CI: 1.04–1.33] per cm), pulmonary (OR: 1.54 [95% CI: 1.34–1.76]), mitral (OR: 1.16 [95% CI: 1.04–1.29]), and aortic (OR: 1.24 [95% CI: 1.06–1.44]) valves. The logistic regression model showed excellent ability to distinguish SCD, recording an area under the receiver-operating characteristic curve (AUC) of 0.839 (95% CI: 0.821–0.858) in the training dataset and ranging from 0.840 to 0.907 in the external validation groups. When pathologists used the model as support, diagnostic performance improved significantly, with elevated AUC ($P = 0.004$) and sensitivity ($P = 0.01$) in identifying SCD. In cases of sudden coronary artery death, the morphology-based model reached an AUC of 0.781 (95% CI: 0.738–0.825). When applied to myocardial infarction detection with features measurable by echocardiography, the model produced an AUC of 0.697 (95% CI: 0.587–0.817). The extensively validated model represents a new supportive instrument that enables pathologists to conduct quantitative SCD evaluations and offers clinicians a promising resource for recognizing myocardial infarction and issuing early warnings for potential SCD events.

Keywords: Sudden cardiac death, Forensic autopsy, Cardiac pathology, Machine learning, Myocardial infarction

How to Cite This Article: De Smet W, Van Dam L, Janssens P. Artificial Intelligence–Enabled Cardiac Lesion Quantification Improves Diagnosis of Sudden Cardiac Death. Interdiscip Res Med Sci Spec. 2026;6(1):15-28. https://doi.org/10.51847/i79E3fMNGZ

Introduction

Sudden cardiac death (SCD) is the ultimate expression of multiple cardiovascular diseases. It causes millions of deaths across the world each year and constitutes a pressing public health issue [1]. Severe coronary artery disease (CAD) underlies roughly 80% of SCD cases with cardiac origins, while other contributors include non-ischemic cardiomyopathies, cardiac inflammation, congenital anomalies, valvular disorders, and electrical abnormalities [2, 3].

Nearly half of SCD victims experience this event as the first noticeable sign of an undiagnosed cardiac condition. Such occurrences complicate both urgent medical response and postmortem evaluation, particularly when prior clinical documentation or trustworthy eyewitness reports are missing [4, 5]. Forensic evaluation of SCD also

differs substantially from clinical approaches, which depend largely on electrocardiographic findings, imaging studies, and biomarkers of early myocardial damage [6]. Traditional biochemical markers have restricted value after death due to autolytic processes, bacterial activity, and postmortem metabolic shifts, especially with postponed sample acquisition [7-9]. Although researchers have identified various potential indicators—including mRNAs, circular RNAs, immunohistochemical markers, proteins, and metabolites [10-14]—these candidates have not yet reached routine application. Challenges include insufficient external validation of early studies and the technical complexity and expense of required assays.

Forensic identification of SCD therefore continues to rest on thorough autopsy procedures. These encompass direct measurement of gross cardiac morphology, microscopic tissue analysis, review of existing medical information, witness statements, and exclusion of alternative causes [15]. However, the absence of consistent criteria for weighing risk factors and pathological findings can lead to variability in conclusions that reflect individual examiners' experience rather than standardized assessment.

This multicenter project developed and externally validated a machine learning (ML) framework grounded in autopsy data for comprehensive cardiac lesion analysis. The objective was to furnish an objective method for confirming SCD and to enhance diagnostic reliability in diverse forensic contexts. Because CAD is the predominant cause of SCD [2, 3] and produces recognizable structural changes in the heart [16-19], the study also explored translation of the autopsy-derived model into clinical practice and examined its utility for identifying myocardial infarction (MI).

Materials and Methods

Study design

Cases of non-criminal deaths were prospectively and consecutively collected from forensic medicine departments at six academic institutions: Sun Yat-sen University (SYSU), Southern Medical University (SMU), Jinan University (JNU), China Medical University (CMU), Guizhou Medical University (GMU), and Xi'an Jiaotong University (XJTU). Eligible cases met the following requirements: (1) individuals aged 16 years or older; (2) performance of a full forensic autopsy incorporating gross inspection, tissue microscopy, biochemical assays, and toxicological analysis, with retention of biological samples. Determination of the cause of death involved consensus evaluation by a minimum of three experienced forensic pathologists (including at least one senior specialist), followed by independent verification from an additional senior expert. This process integrated comprehensive autopsy observations, details of the death scene, and any accessible clinical history. SCD was characterized as an abrupt, unexpected natural death of cardiac origin occurring shortly after symptom onset, with corresponding postmortem cardiac pathology identified and other potential lethal non-cardiac etiologies ruled out. Sudden coronary artery death specifically referred to SCD attributable to CAD. Exclusion occurred in instances where the cause of death could not be definitively established because of incomplete diagnostic information, an inadequate autopsy protocol, or absence of cardiac morphological documentation.

In parallel, a prospective clinical cohort was assembled by sequentially enrolling patients who presented with chest pain and underwent coronary or CT angiography accompanied by echocardiography at the First Affiliated Hospital of Sun Yat-sen University from April to September 2024. The purpose was to examine relationships between cardiac structural parameters and MI. Confirmation of MI was based on a combination of clinical manifestations, electrocardiographic findings, circulating myocardial injury markers, and angiographic evidence. This investigation was conducted in accordance with the Declaration of Helsinki and obtained ethical clearance from the Medical Ethics Committee of Sun Yat-sen University (Approval No. 2024–062) and the First Affiliated Hospital of Sun Yat-sen University (Approval No. 2024–599). Written informed consent was acquired from the next of kin of forensic cases and directly from clinical participants. The study report adheres to the STrengthening the Reporting of OBservational studies in Epidemiology (STROBE) guidelines and the Transparent Reporting of a multivariable prediction model for Individual Prognosis Or Diagnosis (TRIPOD) + artificial intelligence recommendations [20, 21].

Candidate predictors

Examination of the heart was carried out using a conventional inflow-outflow dissection technique consistent with the Forensic medicine–General technical specifications for examination of death (GA/T 147–2019) and the Forensic medicine–Specifications for examination of sudden death (GA/T 170–2019), official public safety

industry standards in the People's Republic of China. Fifteen demographic and gross morphological characteristics were obtained from forensic pathology documentation and considered as potential predictors. Demographic variables consisted of age, sex, stature, and thickness of abdominal subcutaneous adipose tissue. Seven standard cardiac morphological measurements routinely obtained in forensic examinations were included: heart weight, left ventricular wall thickness (LVWT), right ventricular wall thickness (RVWT), and the circumferences of the tricuspid (cTA), pulmonary (cPA), mitral (cMA), and aortic (cAA) valve annuli. Degrees of stenosis in the left anterior descending (LAD), left circumflex (LCX), and right coronary (RCA) arteries were quantified as continuous measures. Presence of MI was determined from macroscopic and microscopic findings [22] and coded as a binary outcome.

Work flow of the model development

As depicted in the Graphical abstract and **Figure 1**, eight distinct machine learning algorithms were employed to generate diagnostic models for SCD detection within the SYSU training dataset. Following hyperparameter optimization, the models were initially tested at the SMU site to identify the most effective algorithm. This selected model then underwent rigorous external validation across the CMU, JNU, GMU, and XJTU cohorts.

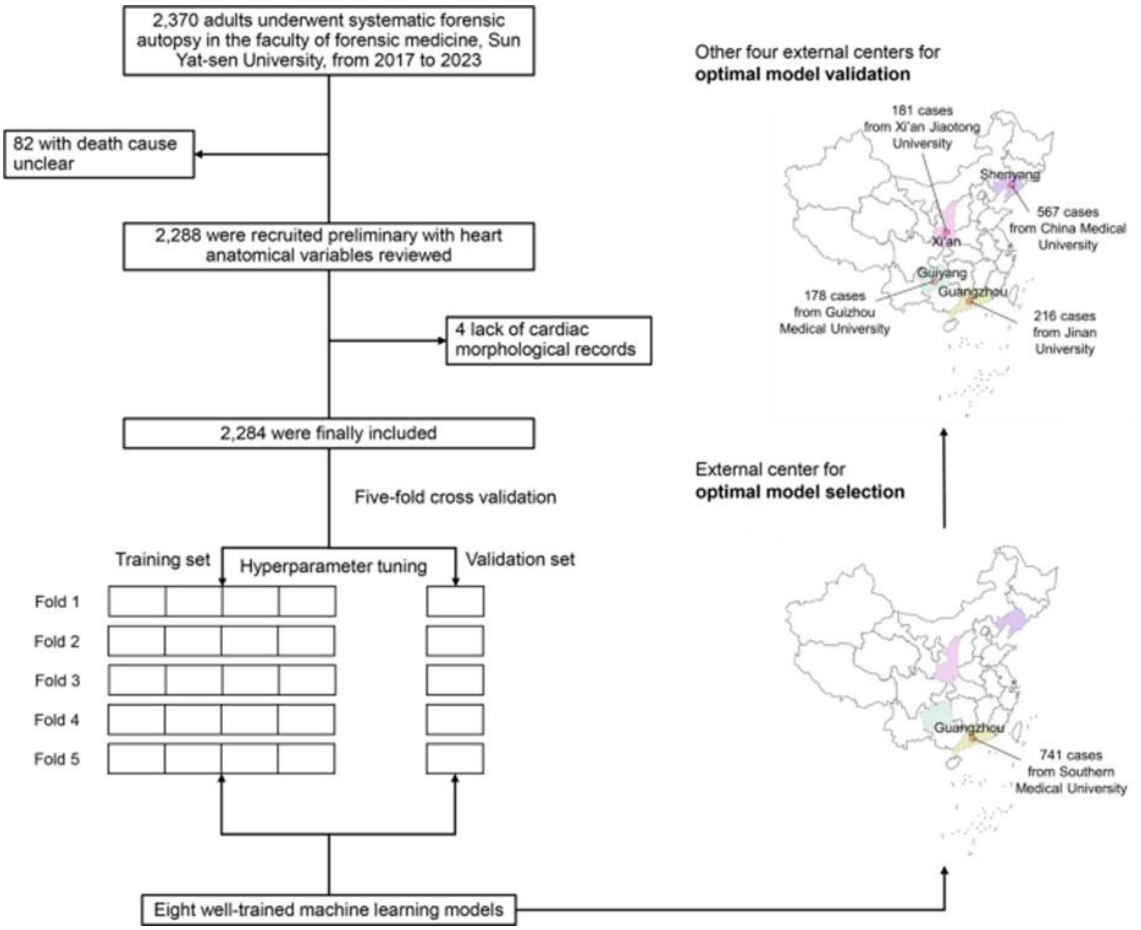

Figure 1. Study flowchart and machine learning model development.

A total of 2284 cases from the Sun Yat-sen University dataset and 1883 cases from the Southern Medical University, China Medical University, Jinan University, Xi'an Jiaotong University, and Guizhou Medical University datasets (showing SCD prevalence of 30.0% and 23.4%, respectively) were utilized for model construction and external validation.

Data processing

Absent data points across the datasets were handled through independent imputation via the missForest algorithm, a non-parametric approach recognized for its effectiveness in managing missing information in complex, mixed-type, and high-dimensional datasets using iterative procedures [23]. Continuous features were standardized based

on the mean and standard deviation derived from the imputed training set, and these parameters were subsequently applied to normalize the other datasets.

Feature selection

Feature selection in the training set was performed using two complementary strategies: least absolute shrinkage and selection operator (LASSO) regression and random forest-based recursive feature elimination (RF-RFE), both implemented with tenfold cross-validation. The common features retained by both approaches served as the final input variables for model building. Assessment of multicollinearity involved variance inflation factor calculations and correlation matrix visualization. To enhance model transparency, SHAP (Shapley Additive exPlanations) values generated from the extreme gradient boosting (XGBoost) framework were calculated to quantify feature contributions and establish importance rankings [24].

Model construction

Eight distinct machine learning approaches, specifically random forest, XGBoost, adaptive boosting trees, logistic regression (LR)-nomogram, support vector machine using a radial basis function kernel, K-nearest neighbor, Gaussian naïve Bayes, and a single-hidden-layer neural network, were employed to generate the predictive models on the training data. Hyperparameter optimization involved grid search coupled with fivefold cross-validation. The tuned models underwent initial assessment within the SMU cohort. The variant demonstrating the superior area under the receiver-operating characteristic curve (AUC) was designated as the primary prediction tool. An accessible interactive online tool was created with ShinyApp for real-time application (available at: https://lich283.shinyapps.io/ML_model_forensic_diagnosis_SCD_sysu/). External testing of the selected model's transportability was performed using data from the CMU, JNU, GMU, and XJTU centers, which represent diverse geographic areas including northeastern, southern, central, and northwestern China.

Model performance appraisal

Comprehensive evaluation of model efficacy was conducted in the training dataset and across the five independent external validation sites. Discriminative power was quantified through receiver-operating characteristic (ROC) curves and associated area under the curve (AUC) metrics. Further indicators of performance—accuracy, sensitivity, specificity, positive predictive value, negative predictive value, F1 score, and Kappa statistic—were derived using the threshold value that maximized Youden's index in the training set.

Human–machine fusion

Given that the model evaluates the extent of cardiac lesions independently of contextual death scene details or alternative lethal factors, a collaborative human–machine framework was developed to better support forensic decision processes. To assess the effectiveness of this integrated strategy, the study recruited four senior forensic pathologists possessing more than 10 years of professional experience and four junior pathologists with over 3 years of experience. The previously unseen XJTU dataset served as the testing material for this experiment. Each pathologist evaluated cases individually and assigned binary classifications relying solely on autopsy-derived information, mirroring typical diagnostic constraints encountered in forensic settings where scene evidence may be limited. Comparative analysis of discriminatory performance between pathologists and the model utilized Delong's test for AUC and McNemar's test for sensitivity and specificity. Subsequently, pathologists received the model-generated SCD probability estimates for each case as well as summary performance statistics from the training and other external datasets (excluding the test set). They were then permitted to reassess and modify their initial judgments if desired. Changes in pathologists' AUC, sensitivity, and specificity following model exposure were examined using one-tailed Wilcoxon signed-rank tests.

Clinical translation

To evaluate the broader applicability of cardiac macro-morphological parameters and machine learning frameworks, an interdisciplinary adaptation was undertaken. This process shifted from postmortem determination of sudden coronary artery death in CAD-related natural fatalities to clinical recognition of MI in symptomatic chest pain patients. Identical feature selection procedures were utilized, with forensic-derived morphological attributes converted into parameters suitable for clinical measurement: valve annulus circumferences were recalculated as diameters measurable by two-dimensional echocardiography per relevant clinical standards [25-

27]. End-diastolic thickness of the left ventricular posterior wall and right ventricular anterior wall was obtained from parasternal long-axis views [27]. A logistic regression model based on these transformed features was developed for MI detection.

Statistics analysis

Categorical data were reported as frequencies and percentages. Continuous data were expressed as means accompanied by standard deviations or as medians with interquartile ranges, selected according to distributional properties. Associations between individual candidate variables and SCD were investigated via univariate and multivariable logistic regression models. All statistical computations, model training, and performance assessments were executed in R software (version 4.3.2).

Results and Discussion

Study population characteristics

Out of 2370 cases initially reviewed in the SYSU cohort spanning 2017 to 2023, 2284 satisfied the inclusion criteria and were retained for analysis **(Figure 1)**. Males comprised 73.7% of the sample, and the average age at death was 46.8 years (standard deviation: 14.9). Natural causes accounted for 73.2% of fatalities, while sudden deaths represented 52.8%. SCD was established in 581 males (34.5%) and 105 females (17.5%), with 58.0% of affected males and 34.3% of affected females lacking any prior medical documentation. The five external centers contributed 1883 cases, 75.3% of whom were male, with a mean age at death of 50.4 years (standard deviation: 15.6). SCD diagnoses included 371 males (26.2%) and 70 females (17.7%). Detailed demographic profiles and cardiac examination findings for the full sample and each individual cohort appear in **Table 1**. Rates of missing data remained under 5% in every dataset.

Table 1. Demographic and heart examination characteristics of study cohorts across six forensic centers From: An autopsy-based cardiac lesion evaluation system facilitates quantitative diagnosis of sudden cardiac death: development and multicenter validation of a machine learning model

Variable	Validation Cohort (Female)		Validation Cohort (Male)		Training Cohort (Female)		Training Cohort (Male)	
	Non-SCD	SCD	Non-SCD	SCD	Non-SCD	SCD	Non-SCD	SCD
Sample size, n	396	70	1046	371	495	105	1103	581
Cases with available medical records, n (%)	262 (66.2)	44 (62.9)	672 (64.2)	194 (52.3)	352 (71.1)	69 (65.7)	652 (59.1)	244 (42.0)
Natural deaths, n (%)	183 (46.2)	—	418 (40.0)	—	350 (70.7)	—	637 (57.8)	—
Sudden deaths, n (%)	92 (23.2)	—	213 (20.4)	—	186 (37.6)	—	334 (30.3)	—
Sudden coronary artery death, n (%)	—	41 (58.6)	—	323 (87.1)	—	42 (40.0)	—	464 (79.9)
Age, years	48.1 ± 17.2	51.9 ± 18.3	50.8 ± 15.7	51.5 ± 12.7	45.4 ± 16.0	50.7 ± 17.6	46.0 ± 14.7	48.8 ± 13.4
Height, cm	157.6 ± 7.0	156.6 ± 7.0	167.6 ± 7.6	168.8 ± 7.5	156.5 ± 6.1	155.7 ± 6.9	167.0 ± 7.1	166.9 ± 6.5
Abdominal subcutaneous fat thickness, cm[b]	2.98 ± 1.25	3.24 ± 1.05	2.12 ± 1.06	2.70 ± 1.12	2.64 ± 1.13	2.71 ± 1.08	1.92 ± 1.10	2.16 ± 0.89
Heart mass, g	315 ± 82	375 ± 100	378 ± 97	457 ± 121	328 ± 79	370 ± 98	385 ± 99	431 ± 106
Coronary artery disease (CAD), n (%)	52 (13.1)	40 (57.1)	314 (30.0)	312 (84.1)	46 (9.3)	38 (36.2)	185 (16.8)	425 (73.1)
Myocardial infarction (MI), n (%)	22 (5.6)	32 (45.7)	88 (8.4)	226 (60.9)	6 (1.2)	26 (24.8)	70 (6.3)	224 (38.6)
Cardiomyopathy, n (%)	6 (1.5)	6 (8.6)	15 (1.4)	29 (7.8)	19 (3.8)	23 (21.9)	71 (6.4)	103 (17.7)
Left ventricular wall thickness, cm	1.22 ± 0.26	1.29 ± 0.23	1.34 ± 0.25	1.43 ± 0.27	1.14 ± 0.16	1.16 ± 0.16	1.26 ± 0.19	1.28 ± 0.20
Right ventricular wall thickness, cm	0.32 ± 0.11	0.35 ± 0.13	0.36 ± 0.12	0.39 ± 0.13	0.29 ± 0.08	0.30 ± 0.09	0.31 ± 0.07	0.32 ± 0.08
Tricuspid annulus circumference, cm	11.23 ± 1.00	11.61 ± 0.98	12.13 ± 1.14	12.53 ± 1.09	10.85 ± 0.70	10.81 ± 1.36	11.62 ± 0.85	11.81 ± 0.77

Pulmonary annulus circumference, cm	7.12 ± 0.92	7.51 ± 1.07	7.73 ± 1.01	7.96 ± 0.96	7.34 ± 0.71	7.54 ± 0.69	7.89 ± 0.79	8.17 ± 0.72
Mitral annulus circumference, cm	8.83 ± 0.92	9.24 ± 1.13	9.64 ± 1.07	10.05 ± 1.06	8.67 ± 0.86	8.63 ± 1.43	9.32 ± 0.93	9.54 ± 0.87
Aortic annulus circumference, cm	6.53 ± 0.83	6.96 ± 0.91	7.26 ± 0.87	7.41 ± 0.83	6.57 ± 0.61	6.68 ± 0.72	7.13 ± 0.72	7.29 ± 0.62

1. Abbreviation: SCD sudden cardiac death, CAD coronary artery disease, MI myocardial infarction

2. aCharacteristics were summarized as frequency with percentage for nominal variable and mean with standard deviation for continuous variable with normal distribution

3. bData of abdominal subcutaneous fat thickness were not available in China Medical University and Guizhou Medical University dataset

Predictive value of candidate variables for the identification of sudden cardiac death

Univariate and multivariate logistic regression analyses were performed on the SYSU dataset to evaluate the predictive capacity of the selected candidate variables **(Table 2)**. Regarding demographic factors, male sex, advanced age, and increased abdominal subcutaneous fat thickness showed significant associations with elevated risk of sudden cardiac death (SCD). The corresponding adjusted odds ratios were 2.49 (95% CI: 1.98–3.16) for male sex, 1.16 per 10-year increment (95% CI: 1.10–1.24) for age, and 1.24 per cm increase (95% CI: 1.14–1.36) for abdominal subcutaneous fat thickness. Additionally, coronary artery disease, myocardial infarction, and cardiomyopathy represented important characteristics linked to SCD. Each 25% increment in the degree of stenosis in the left anterior descending artery, left circumflex artery, and right coronary artery corresponded to a 2.34-fold (95% CI: 2.16–2.55), 2.80-fold (95% CI: 2.42–3.30), and 2.29-fold (95% CI: 2.08–2.53) heightened risk of SCD, respectively. Greater heart weight along with increased left ventricular wall thickness, right ventricular wall thickness, tricuspid annulus circumference, pulmonary annulus circumference, mitral annulus circumference, and aortic annulus circumference were also identified as significant indicators of SCD **(Table 2)**.

Table 2. Univariate and multivariate-adjusted relationships of candidate variables with sudden cardiac death derived from logistic regression modeling

From: An autopsy-based cardiac lesion evaluation system facilitates quantitative diagnosis of sudden cardiac death: development and multicenter validation of a machine learning model

Predictor	P-value	Adjusted Multivariable AnalysisOR (95% CI)[a]	P-value	Unadjusted AnalysisOR (95% CI)
Sex (male vs. female)	< 0.001	2.49 (1.98–3.16)	< 0.001	2.48 (1.97–3.15)
Age (per 10-year increment)	< 0.001	1.16 (1.10–1.24)	< 0.001	1.16 (1.09–1.23)
Body height (per 10-cm increase)	0.632	1.04 (0.90–1.19)	< 0.001	1.24 (1.11–1.38)
Abdominal subcutaneous fat thickness (per cm)	< 0.001	1.24 (1.14–1.36)	0.052	1.08 (1.00–1.17)
Coronary artery disease (CAD)	< 0.001	12.4 (9.9–15.7)	< 0.001	12.3 (10.0–15.2)
Myocardial infarction (MI)	< 0.001	10.5 (7.90–14.1)	< 0.001	11.5 (8.70–15.2)
Degree of LAD stenosis (per 25% increase)	< 0.001	2.34 (2.16–2.55)	< 0.001	2.31 (2.14–2.49)
Degree of LCX stenosis (per 25% increase)	< 0.001	2.80 (2.42–3.30)	< 0.001	2.97 (2.56–3.49)
Degree of RCA stenosis (per 25% increase)	< 0.001	2.29 (2.08–2.53)	< 0.001	2.37 (2.16–2.61)
Cardiomyopathy	< 0.001	3.58 (2.67–4.81)	< 0.001	3.77 (2.83–5.04)
Heart weight (per 100 g increase)	< 0.001	1.53 (1.38–1.71)	< 0.001	1.67 (1.53–1.84)
Left ventricular wall thickness (per mm)	0.237	1.03 (0.98–1.09)	< 0.001	1.13 (1.08–1.18)
Right ventricular wall thickness (per mm)	0.009	1.17 (1.04–1.32)	< 0.001	1.33 (1.18–1.50)
Tricuspid annulus circumference (per cm)	0.013	1.17 (1.04–1.33)	< 0.001	1.43 (1.28–1.59)
Pulmonary annulus circumference (per cm)	< 0.001	1.54 (1.34–1.76)	< 0.001	1.79 (1.59–2.02)
Mitral annulus circumference (per cm)	0.009	1.16 (1.04–1.29)	< 0.001	1.36 (1.23–1.50)
Aortic annulus circumference (per cm)	0.006	1.24 (1.06–1.44)	< 0.001	1.58 (1.39–1.80)

1. Abbreviation: OR odds ratio, CAD coronary artery disease, MI myocardial infarction, LAD left anterior descending artery, LCX left circumflex artery, RCA right coronary artery

2. aThe ORs were adjusted by age and sex for demographic variables and further adjusted by body height and abdominal subcutaneous fat thickness for cardiac morphological variables in multivariate logistic regression models

Model development and optimal model selection

Following data standardization in the SYSU dataset, both LASSO regression **(Figures 2a and 2b)** and random forest-based recursive feature elimination (RF-RFE) **(Figure 2c)** techniques were utilized to perform feature selection. The two methods yielded eight and thirteen variables, respectively. The eight variables common to both approaches were adopted as the final candidate set **(Figure 2d)**. Their ranked importance was as follows: LAD, age, heart weight, RCA, MI, LVWT, LCX, and cPA **(Figure 2e)**. Assessment confirmed the absence of multicollinearity within this selected variable set.

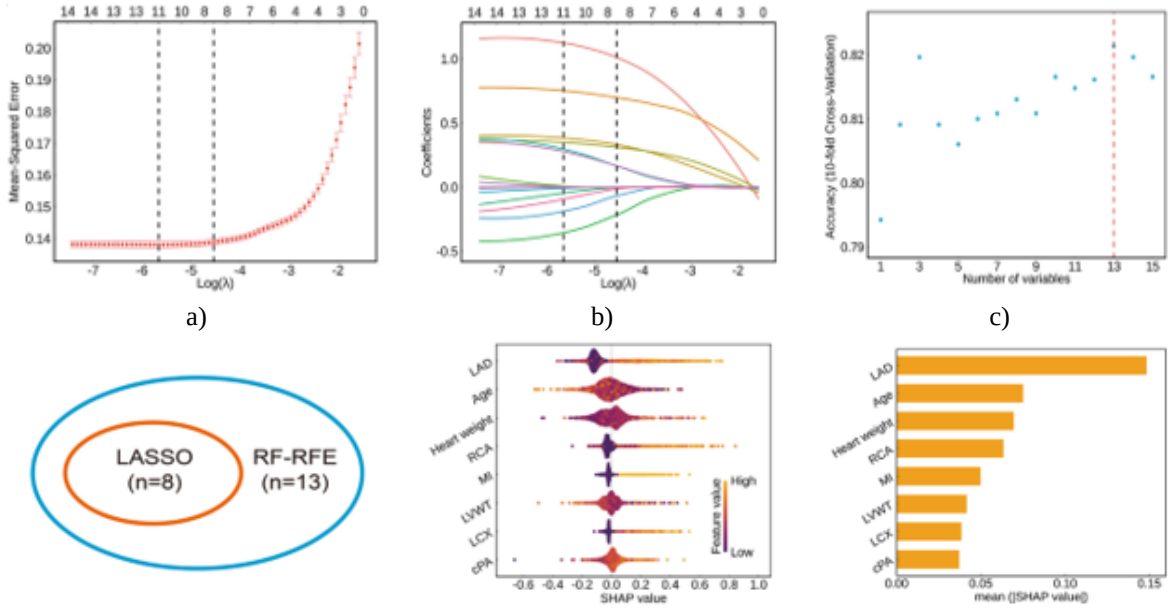

a) b) c)

d) e) f)

Figure 2. Feature selection process for SCD prediction in the SYSU dataset (n = 2284).

A Plot displaying mean squared error against log (λ) for the LASSO regression model under tenfold cross-validation. Dotted vertical lines mark the optimal values based on the minimum criteria (left) and the one-standard-error criterion (right, chosen as the optimal penalty parameter). B Coefficient paths from LASSO regression. Each curve tracks the coefficient of an individual feature as the regularization parameter (λ) changes, with different colors used to distinguish variables. At the selected optimal λ, eight variables (age, LAD, LCX, RCA, MI, heart weight, LVWT, and cPA) retained non-zero coefficients. C Scatter plot of model accuracy versus the number of selected features in RF-RFE using tenfold cross-validation. The red dotted vertical line highlights the optimal number of variables (n = 13, comprising age, abdominal subcutaneous fat thickness, LAD, LCX, RCA, MI, heart weight, LVWT, RVWT, cAA, cPA, cMA, and cTA) that produced peak accuracy. D Venn diagram showing the intersection of variables chosen by LASSO and RF-RFE. E SHAP-based explanation of feature contributions to SCD prediction. Higher SHAP values for a given feature indicate greater influence toward an SCD diagnosis. The graduated yellow color scale reflects higher feature values. F Variable importance ranking according to the mean absolute SHAP value. Abbreviation: LASSO, least absolute shrinkage and selection operator; RF-RFE, recursive feature elimination based on random forest; LAD, left anterior descending artery; LCX, left circumflex artery; RCA, right coronary artery; MI, myocardial infarction; LVWT, left ventricle wall thickness; RVWT, right ventricle wall thickness; cTA, circumference of tricuspid annulus; cPA, circumference of pulmonary annulus; cMA, circumference of mitral annulus; cAA, circumference of aortic annulus; SHAP, Shapley Additive exPlanations

Eight machine learning algorithms were trained on the SYSU dataset, producing AUC values between 0.702 (K-nearest neighbor) and 0.866 (XGBoost) **(Figure 3a)**. Applying the optimal threshold determined by the highest Youden's index, the accuracy of these models ranged from 0.692 (K-nearest neighbor) to 0.827 (single-hidden-layer neural network). In the independent SMU validation cohort, AUC values varied from 0.590 (K-nearest neighbor) to 0.840 (logistic regression), resulting in the selection of logistic regression as the final diagnostic model **(Figure 3b)**. A nomogram was generated from the logistic regression model **(Figure 3c)** and supplemented with an online web calculator for practical use.

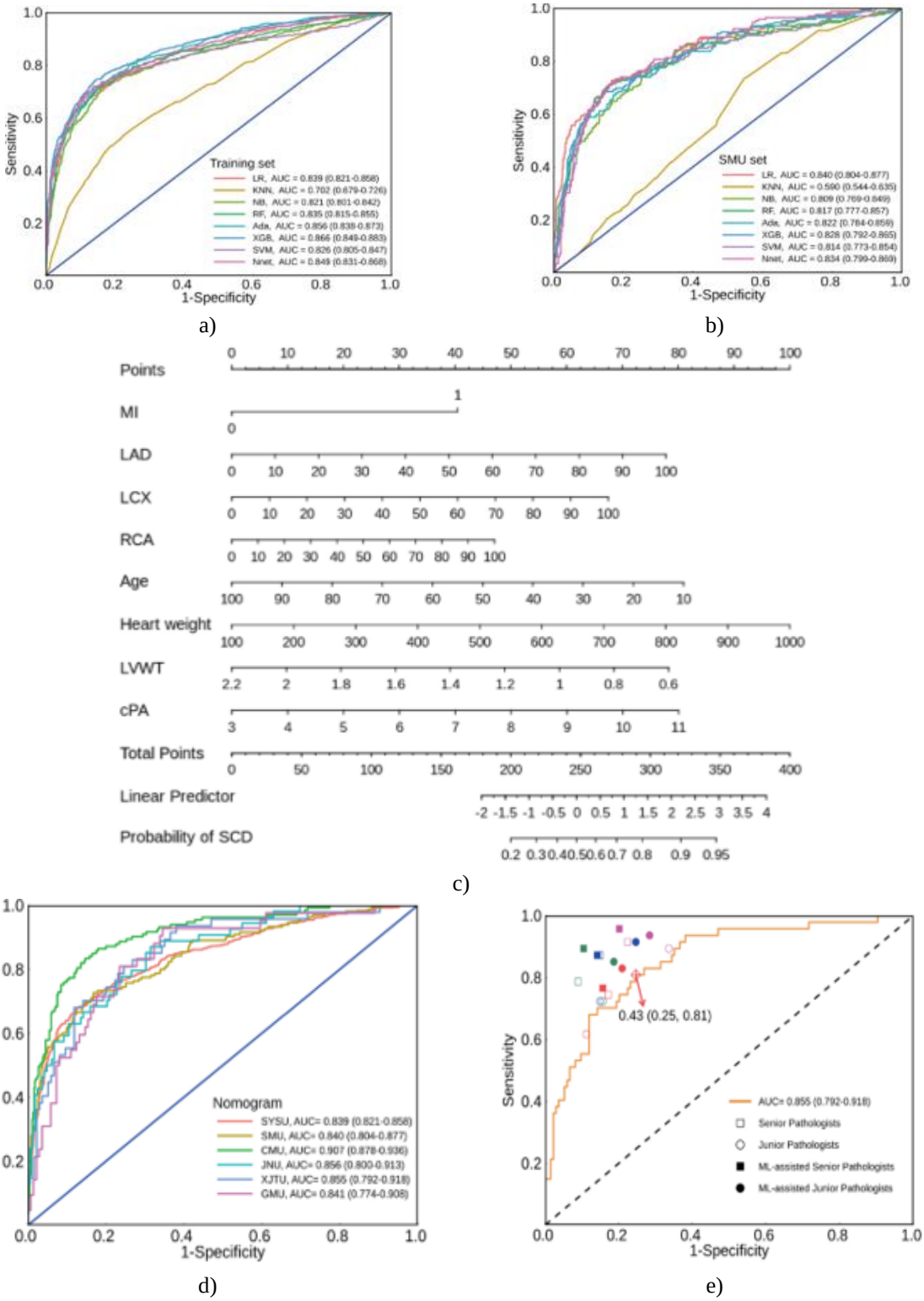

Figure 3. Development, validation, and human–machine integration of models for sudden cardiac death prediction.

a) ROC curves for the eight machine learning models in the training cohort (n = 2284). b) ROC curves for the eight machine learning models in the SMU validation cohort (n = 741). c) Nomogram constructed based on the logistic regression model. d) ROC curves demonstrating nomogram performance across the SYSU, SMU (n = 741), JNU (n = 216), CMU (n = 567), GMU (n = 178), and XJTU (n = 181) datasets. e) Results of the human–machine comparison and collaborative experiment conducted in the XJTU dataset (n = 181). Squares and circles denote senior and junior pathologists, respectively. Distinct colors identify individual pathologists. Hollow markers represent unaided performance, while solid markers indicate performance with

nomogram support. Abbreviation: LR, logistic regression; KNN, K-nearest neighbor; NB, Naïve Bayes; RF, random forest; Ada, Adaboost; XGB, XGBoost; SVM, support vector machine; Nnet, single-hidden-layer neural network; MI, myocardial infarction; LAD, left anterior descending artery; LCX, left circumflex artery; RCA, right coronary artery; LVWT, left ventricle wall thickness; cPA, circumference of pulmonary annulus

Multicenter external validation of the model

The developed nomogram was subjected to external validation in four independent forensic institutions situated in distinct Chinese provinces. The tool exhibited consistently strong discriminatory power, attaining AUC values of 0.907 (95% CI: 0.878–0.936) in the CMU dataset, 0.856 (95% CI: 0.800–0.913) in the JNU dataset, 0.855 (95% CI: 0.792–0.918) in the XJTU dataset, and 0.841 (95% CI: 0.774–0.908) in the GMU dataset **(Figure 3d)**. Setting the predicted probability threshold at 0.36, determined via the highest Youden's index, produced an accuracy of 81.5%, sensitivity of 68.1%, and specificity of 87.3% within the SYSU training cohort. Across the external validation sites, accuracy varied between 72.6% and 82.0%, sensitivity between 66.7% and 86.5%, and specificity between 70.9% and 83.8%.

Sensitivity analyses and subgroup evaluations

The effect of missing data on overall model efficacy was initially assessed by reconstructing the nomogram in the training set using only complete cases. This complete-case analysis yielded an AUC of 0.845 (95% CI: 0.826–0.864) in the training data and values ranging from 0.831 to 0.905 in the external validation cohorts, closely mirroring the outcomes observed with the original imputed data.

The nomogram's utility was next examined in two distinct forensic contexts simulating practical casework. These included populations classified as natural deaths (where non-cardiac exogenous causes had been effectively ruled out through available witness statements and standard postmortem examinations) and sudden deaths (incorporating additional information from witnessed events). The model maintained good predictive accuracy in both settings, with an AUC of 0.818 (95% CI: 0.797–0.839) for natural death cases and 0.814 (95% CI: 0.791–0.838) for sudden death cases. Corresponding AUC ranges in the external centers were 0.802 (SMU) to 0.874 (CMU) for natural deaths and 0.801 (SMU) to 0.906 (CMU) for sudden deaths.

Additional subgroup analyses explored performance stratified by underlying disease categories. The nomogram demonstrated moderate discriminative ability among individuals with coronary artery disease (AUC 0.758, 95% CI: 0.733–0.783) and cardiomyopathy (AUC 0.645, 95% CI: 0.580–0.710).

Human–machine collaborative assessment

To determine the clinical applicability of the nomogram, a comparative study involving pathologists with and without model support was performed using the XJTU dataset. Without assistance, senior pathologists achieved AUC values between 0.787 and 0.862, whereas junior pathologists ranged from 0.753 to 0.787, revealing a statistically significant difference [P = 0.02]. The nomogram alone exceeded the diagnostic performance of every junior pathologist and three out of four senior pathologists. Integration of the nomogram led to meaningful enhancements in both AUC and sensitivity for senior pathologists [P = 0.004] and junior pathologists [P = 0.01] **(Figure 3e)**. Notably, one senior and three junior pathologists experienced substantial gains in sensitivity, and half of the junior pathologists also recorded improved specificity.

Clinical application and translation

Within the SYSU dataset (n = 530), LASSO regression and RF-RFE procedures were once again employed to identify relevant features, resulting in the selection of eight variables by LASSO and eleven by RF-RFE. The common variables retained from both techniques—RCA, LAD, LCX, age, LVWT, RVWT, cPA, and sex—were ranked according to their contribution **(Figure 4a)**. When these were entered into a logistic regression framework, the model displayed acceptable ability to forecast sudden coronary artery death, reaching an AUC of 0.781 (95% CI: 0.738–0.825) internally in the SYSU cohort. External testing in additional forensic centers produced AUCs spanning from 0.578 to 0.796 **(Figure 4b)**.

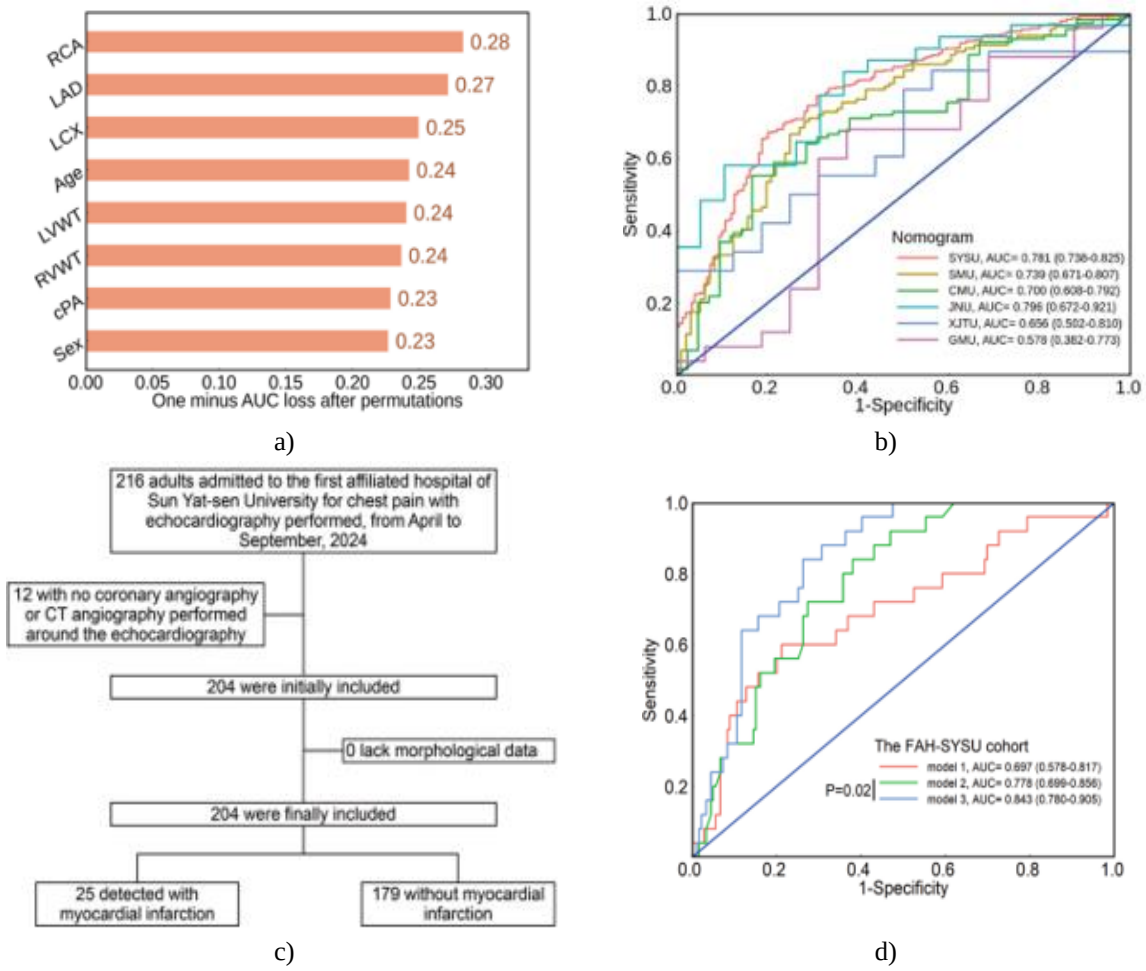

Figure 4. Cross-disciplinary translation linking forensic identification of sudden coronary artery death in subjects affected by coronary artery disease with clinical forecasting of myocardial infarction in individuals suffering from chest pain. A) Assessment of variable importance through single-permutation analysis in the logistic regression model for the shared features derived from LASSO and RF-RFE, employing 1-AUC as the loss function. Variables causing larger declines in performance are deemed more influential. b) ROC curves illustrating the logistic regression model's performance in diagnosing sudden coronary artery death across the SYSU (n = 530), SMU (n = 210), JNU (n = 50), CMU (n = 156), GMU (n = 41), and XJTU (n = 54) datasets. c) Schematic overview of patient enrollment and progression in the clinical cohort at the First Affiliated Hospital of Sun Yat-sen University. d) ROC curves depicting the logistic regression model for predicting myocardial infarction within the clinical population (n = 204).

Model 1 combined sex, age, and echocardiography parameters adapted from the forensic data, specifically thickness of the left ventricular posterior wall, right ventricular anterior wall, and pulmonary valve diameter. Model 2, used as the baseline comparator, contained solely the degree of stenosis in the LAD, LCX, and RCA. Model 3 incorporated the complete set of adapted variables from the LASSO–RF-RFE overlap, including stenosis severity in the LAD, LCX, and RCA as well as sex, age, left ventricular posterior wall thickness, right ventricular anterior wall thickness, and pulmonary valve diameter. Statistical comparison of Model 2 versus Model 3 utilized a one-tailed DeLong's test. Abbreviation: LVWT, left ventricle wall thickness; RVWT, right ventricle wall thickness; cPA, circumference of pulmonary annulus; LAD, stenosis degree of left anterior descending artery; LCX, stenosis degree of left circumflex artery; RCA, stenosis degree of right coronary artery; LASSO, least absolute shrinkage and selection operator; RF-RFE, recursive feature elimination based on random forest

The clinical investigation involved 204 patients who presented with chest pain, among whom 189 (92.6%) underwent coronary angiography. Myocardial infarction was identified in 25 cases (12.3%) **(Figure 4c)**. Variables originating from the forensic analysis that could be translated into echocardiographic equivalents were examined. Left ventricular posterior wall thickness proved significantly elevated among those with myocardial infarction

(10.32 ± 1.52 mm vs. 9.64 ± 1.34 mm, [P = 0.02]). A logistic regression model built with age, sex, and the measurable echocardiographic features—including left ventricular posterior wall thickness, right ventricular anterior wall thickness, and pulmonary valve diameter—achieved an AUC of 0.697 (95% CI: 0.578–0.817) for detecting myocardial infarction. Adding the morphological characteristics resulted in a marked enhancement relative to a model limited to coronary stenosis measurements alone (0.843 [95% CI: 0.780–0.905] vs. 0.778 [95% CI: 0.669–0.856], [P = 0.02], **(Figure 4d)**).

This investigation assembled a comprehensive autopsy dataset and established a standardized machine learning model grounded in postmortem examinations to enable quantitative assessment of sudden cardiac death (SCD). Following thorough optimization, the model exhibited robust performance within the training cohort, demonstrated reliable generalizability when tested across distinct forensic institutions, and proved effective when integrated into human–machine collaborative diagnostic workflows. In addition, translating autopsy-derived morphological insights into clinical echocardiographic correlates further substantiated the capacity of this morphology-oriented approach to detect myocardial infarction.

Diagnosing SCD in out-of-hospital settings remains exceptionally difficult during forensic inquiries when medical histories and witness testimonies are unavailable. Pathologists frequently differ in their final determinations due to the absence of a consistent, standardized method for evaluating cardiac abnormalities. To address this limitation, the current study introduced an autopsy-driven machine learning system designed to quantify the extent of cardiac pathology, thereby supporting more accurate SCD classification in forensic environments with restricted resources. A logistic regression-based nomogram constructed from eight key variables displayed strong predictive capability in the development dataset and maintained consistent performance at five independent external sites spanning four major provinces in China. Relying exclusively on standard autopsy measurements, this validated model can help estimate the likelihood of SCD in situations where corroborative external evidence is minimal. Additional subgroup evaluations focusing on natural deaths and sudden fatalities reinforced the framework's stability across a wide range of forensic case types. Overall, the nomogram reached diagnostic accuracy on par with experienced senior pathologists (exceeding 10 years of practice) and produced notable gains in both accuracy and sensitivity for practitioners at all experience levels, establishing its utility as a practical assistive tool for clinical decision-making.

In the course of a thorough sequential autopsy, SCD is established once natural cardiac pathologies are identified and potentially lethal non-cardiac conditions are ruled out. A broad spectrum of cardiovascular alterations may precipitate either electrical or mechanical forms of SCD by affecting the coronary arteries, myocardium, valvular structures, conduction pathways, and associated components [3]. These elements remain central to both gross and microscopic inspections. Beyond overtly fatal lesions, certain anatomical traits have been recognized as relevant to SCD risk, such as abdominal fat accumulation, overall heart weight, left ventricular wall thickness (LVWT), and the circumferences of the cardiac valves [28-32]. Such characteristics can furnish additional supportive evidence, especially when hallmark fatal findings are lacking. The principal difficulty involves determining the relative diagnostic importance and weighting of these individual factors within any specific case. Therefore, an integrated analytical framework is essential—one that encompasses not only the most critical lesions but also incorporates supplementary anatomical details that may coexist.

Leveraging a collection of over four thousand meticulously verified cases, the constructed and independently validated system highlighted the diagnostic relevance of morphological and histopathological characteristics, offering meaningful assistance in SCD evaluation. Practically, the tool generates a numerical probability of SCD for each case, allowing pathologists to compare this value against predefined thresholds when reaching a conclusion. This process preserves favorable metrics of accuracy, sensitivity, specificity, negative predictive value, and positive predictive value. The high-sensitivity configuration of the nomogram, in particular, appears promising for lowering missed diagnoses, consistent with outcomes observed in the human–machine integration assessment. The system further benefits from strong interpretability and operational simplicity. By assigning empirically derived weights to histopathological observations, demographic information, and macroscopic features, and by employing SHAP analysis to delineate variable importance and individual contributions, the model enables clearer understanding of each factor's role. This facilitates reasoned diagnostic judgments even in multifaceted presentations involving multiple comorbidities—for instance, simultaneous narrowing across several coronary branches without accompanying fatal histopathological findings. To enhance accessibility, the logistic regression nomogram has been deployed as a web-based platform, providing pathologists with rapid, convenient estimates of SCD probability through an intuitive online calculator.

To enhance applicability in out-of-hospital settings and broaden its clinical relevance, the present model focuses primarily on cardiac lesions and incorporates only routinely available variables. Nevertheless, because the model relies exclusively on standard autopsy observations, a small proportion of autopsy-negative SCD cases may be misclassified, underscoring the need for supplementary advanced techniques such as premortem monitoring, genetic testing, and specialized histopathological analyses [33, 34]. Consequently, the cardiac morphology-based nomogram should be regarded as a supportive instrument in forensic practice, with the definitive diagnosis formulated through comprehensive evaluation of all autopsy results, differential diagnostic information, and any additional required investigations.

Beyond postmortem diagnosis, the prevention of SCD constitutes a major unresolved challenge in global cardiovascular medicine [1]. Over recent decades, both left and right ventricular hypertrophy have been shown to be associated with elevated risk of cardiovascular mortality [17, 19]. Despite this, clinically feasible risk-prediction models that integrate cardiac morphological characteristics remain insufficiently developed, even though they hold considerable promise [35, 36]. Given that SCD represents the terminal manifestation of various cardiac conditions, the current model—constructed from forensic autopsy data with cardiac morphological variables and SCD as the endpoint—may offer valuable insights into overall cardiac burden and help identify individuals at elevated risk of SCD. To explore its clinical applicability, we prospectively evaluated a pilot cohort by adapting the forensic autopsy-derived model for use with clinical echocardiography in detecting myocardial infarction (MI), which underlies the majority of SCD events. Patients with MI exhibited increased left ventricular posterior wall thickness, and the composite of morphological variables transformed from anatomical to echocardiographic measurements achieved moderate performance in MI identification. As a noninvasive, inexpensive, and widely accessible bedside imaging modality, echocardiography has demonstrated prognostic value for early risk stratification following acute MI [35]. These initial results indicate that echocardiography-derived morphological parameters can facilitate rapid and quantitative assessment of cardiac burden and may improve MI risk stratification, especially when integrated with conventional risk factors (e.g., blood pressure, diabetes, dyslipidemia, and family history) [37, 38]. Furthermore, the encouraging outcomes in the clinical echocardiography cohort highlight the feasibility of a virtual autopsy approach, whereby morphology-based models are adapted to imaging-based technologies, potentially reducing the necessity for conventional autopsies in the forensic evaluation of SCD.

Several limitations should be acknowledged. First, the diagnostic model functions primarily as a cardiac lesion evaluation tool aimed at improving generality in out-of-hospital diagnosis and expanding its clinical relevance. The presence of competing injuries or diseases may result in occasional false-positive classifications, thereby reducing overall specificity. Second, the nomogram's performance in cases involving uncommon cardiac lesions (such as myocardial inflammation or conduction system abnormalities) has not been comprehensively validated, warranting dedicated investigations focused on these specific causes of death. Third, since the study included cases exclusively from Chinese forensic centers, the morphological characteristics observed in other ethnic populations require further elucidation, and additional validation with appropriate model calibration across diverse ethnic groups is necessary prior to broader international implementation. Finally, the relatively small sample size of the clinical validation cohort limited statistical power for identifying associations with less frequent clinical features, highlighting the need for larger-scale investigations. A comprehensive multicenter cohort study is already planned to confirm the predictive utility of these echocardiography-accessible cardiac morphological parameters.

Conclusion

This multicenter investigation developed and validated a machine learning system based on autopsy data for the evaluation of cardiac lesions. The model exhibited strong performance in SCD diagnosis across varied forensic contexts, achieving accuracy comparable to that of senior pathologists. Human–machine fusion experiments further confirmed its value as an assistive tool. In addition, the morphology-based model, when adapted for clinical use, demonstrated moderate performance in the identification of myocardial infarction within a pilot prospective non-randomized cohort.

Acknowledgments: None

Conflict of Interest: None

Financial Support: None

Ethics Statement: None

References

1. Marijon E, Garcia R, Narayanan K, Karam N, Jouven X. Fighting against sudden cardiac death: need for a paradigm shift-adding near-term prevention and pre-emptive action to long-term prevention. Eur Heart J. 2022;43(15):1457–64.
2. Deo R, Albert CM. Epidemiology and genetics of sudden cardiac death. Circulation. 2012;125(4):620–37.
3. Kandala J, Oommen C, Kern KB. Sudden cardiac death. Br Med Bull. 2017;122(1):5–15.
4. Khairy P, Silka MJ, Moore JP, DiNardo JA, Vehmeijer JT, Sheppard MN, et al. Sudden cardiac death in congenital heart disease. Eur Heart J. 2022;43(22):2103–15.
5. Stecker EC, Vickers C, Waltz J, Socoteanu C, John BT, Mariani R, et al. Population-based analysis of sudden cardiac death with and without left ventricular systolic dysfunction: two-year findings from the Oregon Sudden Unexpected Death Study. J Am Coll Cardiol. 2006;47(6):1161–6.
6. Vogel B, Claessen BE, Arnold SV, Chan D, Cohen DJ, Giannitsis E, et al. ST-segment elevation myocardial infarction. Nat Rev Dis Primers. 2019;5(1):39.
7. Barberi C, van den Hondel KE. The use of cardiac troponin T (cTnT) in the postmortem diagnosis of acute myocardial infarction and sudden cardiac death: a systematic review. Forensic Sci Int. 2018;292:27–38.
8. Palmiere C, Tettamanti C, Bonsignore A, De Stefano F, Vanhaebost J, Rousseau G, et al. Cardiac troponins and NT-proBNP in the forensic setting: overview of sampling site, postmortem interval, cardiopulmonary resuscitation, and review of the literature. Forensic Sci Int. 2018;282:211–8.
9. Xu C, Zhang T, Zhu B, Cao Z. Diagnostic role of postmortem CK-MB in cardiac death: a systematic review and meta-analysis. Forensic Sci Med Pathol. 2020;16(2):287–94.
10. Son GH, Park SH, Kim Y, Kim JY, Kim JW, Chung S, et al. Postmortem mRNA expression patterns in left ventricular myocardial tissues and their implications for forensic diagnosis of sudden cardiac death. Mol Cells. 2014;37(3):241–7.
11. Tian M, Cao Z, Pang H. Circular RNAs in Sudden Cardiac Death Related Diseases: Novel Biomarker for Clinical and Forensic Diagnosis. Mol. 2021;26(4):1155. doi:10.3390/molecules26041155
12. Isailă OM, Ion OM, Luta R, Catinas R, Ionita A, Haisan D, et al. Postmortem Immunohistochemical Findings in Early Acute Myocardial Infarction: A Systematic Review. Int J Mol Sci. 2024;25(14):7625. doi:10.3390/ijms25147625
13. Lin X, Lin Z, Zhao X, Liu Z, Xu C, Yu B, et al. Serum SELENBP1 and VCL Are Effective Biomarkers for Clinical and Forensic Diagnosis of Coronary Artery Spasm. Int J Mol Sci. 2022;23(21):13266. doi:10.3390/ijms232113266
14. Cao J, Wei X, Liu M-F, An G-S, Li J, Du Q-X, et al. Forensic identification of sudden cardiac death: a new approach combining metabolomics and machine learning. Anal Bioanal Chem. 2023;415(12):2291–305.
15. Basso C, Aguilera B, Banner J, Cohle S, d'Amati G, de Gouveia RH, et al. Guidelines for autopsy investigation of sudden cardiac death: 2017 update from the Association for European Cardiovascular Pathology. Virchows Arch. 2017;471(6):691–705.
16. Narayanan K, Reinier K, Teodorescu C, Uy-Evanado A, Aleong R, Chugh H, et al. Left ventricular diameter and risk stratification for sudden cardiac death. J Am Heart Assoc. 2014;3(5):e001193.
17. Kawel-Boehm N, Kronmal R, Eng J, Folsom A, Burke G, Carr JJ, et al. Left ventricular mass at MRI and long-term risk of cardiovascular events: the multi-ethnic study of atherosclerosis (MESA). Radiology. 2019;293(1):107–14.
18. Bluemke DA, Kronmal RA, Lima JA, Liu K, Olson J, Burke GL, et al. The relationship of left ventricular mass and geometry to incident cardiovascular events: the MESA (multi-ethnic study of atherosclerosis) study. J Am Coll Cardiol. 2008;52(25):2148–55.

19. Kawut SM, Barr RG, Lima JA, Praestgaard A, Johnson WC, Chahal H, et al. Right ventricular structure is associated with the risk of heart failure and cardiovascular death: the Multi-Ethnic Study of Atherosclerosis (MESA)–right ventricle study. Circulation. 2012;126(14):1681–8.
20. von Elm E, Altman DG, Egger M, Pocock SJ, Gøtzsche PC, Vandenbroucke JP. The strengthening the reporting of observational studies in epidemiology (STROBE) statement: guidelines for reporting observational studies. Lancet. 2007;370(9596):1453–7.
21. Collins GS, Moons KGM, Dhiman P, Riley RD, Beam AL, Van Calster B, et al. Tripod+AI statement: updated guidance for reporting clinical prediction models that use regression or machine learning methods. BMJ. 2024;385:e078378.
22. Michaud K, Basso C, d'Amati G, Giordano C, Kholová I, Preston SD, et al. Diagnosis of myocardial infarction at autopsy: AECVP reappraisal in the light of the current clinical classification. Virchows Arch. 2020;476(2):179–94.
23. Stekhoven DJ, Bühlmann P. Missforest–non-parametric missing value imputation for mixed-type data. Bioinformatics. 2012;28(1):112–8.
24. Lundberg SM, Lee SI. A unified approach to interpreting model predictions. Adv Neural Inf Process Syst. 2017:4765–74.
25. Zaidi A, Oxborough D, Augustine DX, Bedair R, Harkness A, Rana B, et al. Echocardiographic assessment of the tricuspid and pulmonary valves: A practical guideline from the British Society of Echocardiography. Echo Res Pract. 2020;7(4):G95–122. doi:10.1530/ERP-20-0033
26. Nordblom P, Bech-Hanssen O. Reference values describing the normal mitral valve and the position of the papillary muscles. Echocardiography. 2007;24(7):665–72.
27. Lang RM, Badano LP, Mor-Avi V, Afilalo J, Armstrong A, Ernande L, et al. Recommendations for cardiac chamber quantification by echocardiography in adults: an update from the American Society of Echocardiography and the European Association of Cardiovascular Imaging. Eur Heart J Cardiovasc Imaging. 2015;16(3):233–70.
28. O'Mahony C, Jichi F, Monserrat L, Ortiz-Genga M, Anastasakis A, Rapezzi C, et al. Inverted U-shaped relation between the risk of sudden cardiac death and maximal left ventricular wall thickness in hypertrophic cardiomyopathy. Circ Arrhythm Electrophysiol.2016;9(6):e003818.
29. Zhang L, Tester DJ, Lang D, Chen Y, Zheng J, Gao R, et al. Does sudden unexplained nocturnal death syndrome remain the autopsy-negative disorder: a gross, microscopic, and molecular autopsy investigation in Southern China. Mayo Clin Proc. 2016;91(11):1503–14.
30. Aune D, Schlesinger S, Norat T, Riboli E. Body mass index, abdominal fatness, and the risk of sudden cardiac death: A systematic review and dose-response meta-analysis of prospective studies. Eur J Epidemiol. 2018;33(8):711–22.
31. Garland J, Kesha K, Glenn C, Stables S, Ondruschka B, Lohner L, et al. Heart weight is an independent factor associated with, but is a poor predictor for, sudden cardiac death. Am J Forensic Med Pathol. 2022;43(1):18–22.
32. Altin I, Oruc M, Celbis O, Turkmen Samanci E. Comparison of cardiac wall thicknesses and coronary artery obstructions between deaths resulting from acute myocardial infarction and deaths from other causes. Meden Med J. 2022;37(3):220–5.
33. Guo L, Torii S, Fernandez R, Braumann RE, Fuller DT, Paek KH, et al. Genetic variants associated with unexplained sudden cardiac death in adult White and African American individuals. JAMA Cardiol. 2021;6(9):1013–22.
34. Raju H, Parsons S, Thompson TN, Morgan N, Zentner D, Trainer AH, et al. Insights into sudden cardiac death: exploring the potential relevance of non-diagnostic autopsy findings. Eur Heart J. 2019;40(10):831–8.
35. Prastaro M, Pirozzi E, Gaibazzi N, Paolillo S, Santoro C, Savarese G, et al. Expert Review on the Prognostic Role of Echocardiography after Acute Myocardial Infarction. J Am Soc Echocardiogr. 2017;30(5):431–43.
36. Peek N, Hindricks G, Akbarov A, Tijssen JGP, Jenkins DA, Kapacee Z, et al. Sudden cardiac death after myocardial infarction: individual participant data from pooled cohorts. Eur Heart J. 2024;45(43):4616–26.
37. Lindblad U, Råstam L, Rydén L, Ranstam J, Isacsson SO, Berglund G. Control of blood pressure and risk of first acute myocardial infarction: Skaraborg hypertension project. BMJ. 1994;308(6930):681–6.
38. Reeh J, Therming CB, Heitmann M, Højberg S, Sørum C, Bech J, et al. Prediction of obstructive coronary artery disease and prognosis in patients with suspected stable angina. Eur Heart J. 2019;40(18):1426–35.